Supporting Information

Structure–activity Relationship of the $CuO–CeO_2$ in the Synthesis of Methyl N-Phenylcarbamate

Lu Ji [a] , Conghui Che [a], Fang Li [a, b, *], Wei Xue [a, b], Xiaoshu Ding [a, c], Dongsheng Zhang [a, c] , Jing Li [d, *], Xinqiang Zhao [a, b], Yanji Wang [a, b, c, *]

[a] Hebei Provincial Key Laboratory of Green Chemical Technology and High Efficient Energy Saving, School of Chemical Engineering and Technology, Hebei University of Technology, Tianjin 300401, China

[b] Tianjin Key Laboratory of Chemical Process Safety, Tianjin 300130, China

[c] Hebei Industrial Technology Research Institute of Green Chemical Industry, Huanghua 061100, Hebei, China

[d] School of Civil Engineering, Hebei University of Technology, Tianjin 300401

S1. Experimental section

1.1. Raw material

aniline (98%, Macklin); dimethyl carbonate (98.0%, Macklin); nitrobenzene (98.0%, Sinopharm); Methyl *N*-Phenylcarbamate (98.0%, Macklin); *N*-methylaniline (98.0%, Macklin); *N,N'*-dimethylaniline (98.0%, Rhawn); diphenylurea (98.0%, Macklin). All reagents were used as received without further purification.

1.2. Analytical methods

The internal standard method was used for the quantitative analysis of the products. The internal standard is nitrobenzene. Chromatographic conditions were as follows: Kromasil TM C18 (250 mm×4.6 mm, 5 μm) chromatographic column was used at the flow rate of 0.4 mL/min. The detection wavelength was 254 nm and CH_3OH/H_2O (60/40, V/V) was used as the mobile phase.

S2. N_2 adsorption-desorption isotherms and pore size curves for diverse catalysts

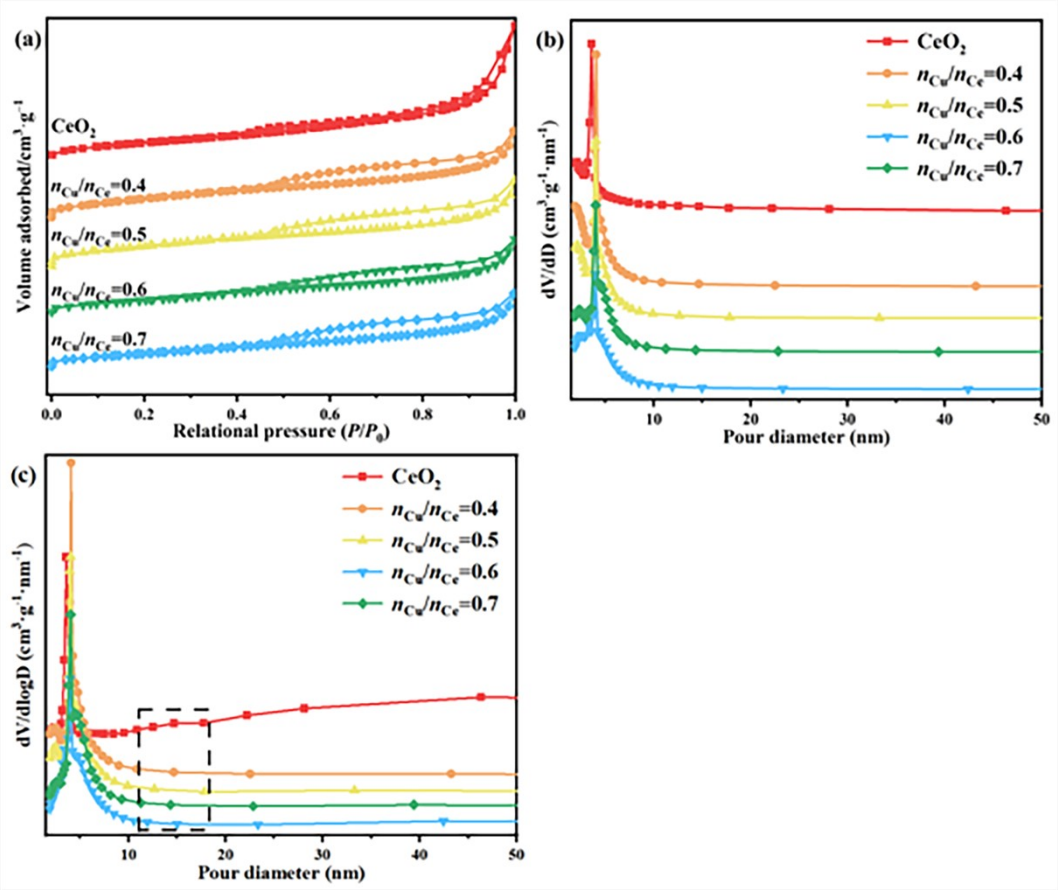

Fig. S1. N_2 adsorption-desorption isotherms (a) ; pore size curves (Y-axis:dV/dD) (b) and pore size curves (Y-axis: dV/dlogD) (c) for diverse catalysts

S3. TEM images and particle size distribution

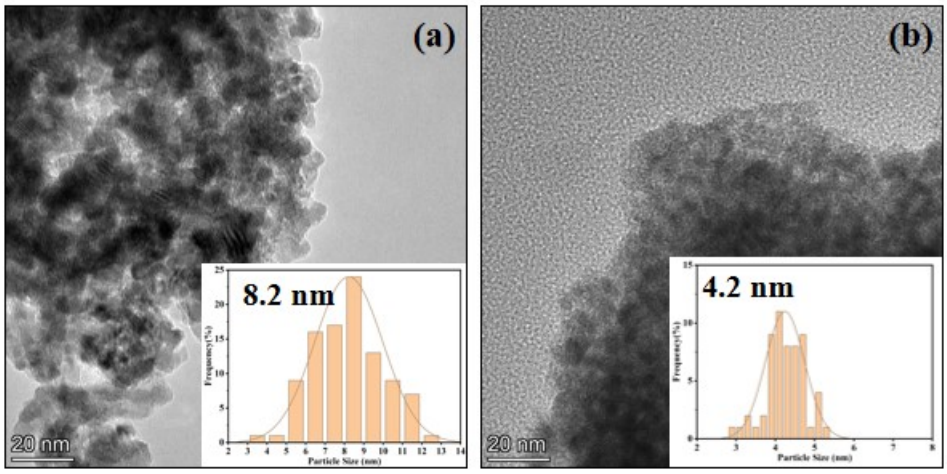

Fig. S2. TEM images and particle size distribution of CeO_2 (a) and CuO–CeO_2 (n_{Cu}/n_{Ce}= 0.6) (b).

S4. Raman

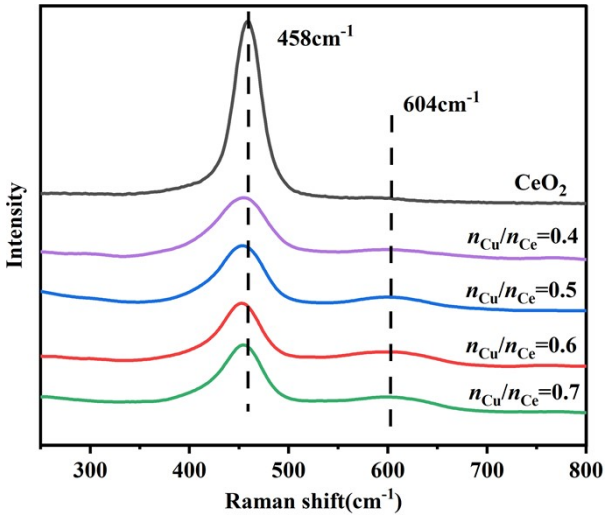

Fig. S3. Raman spectroscopy of different n_{Cu}/n_{Ce} catalysts

Table S1 Characterization result of different catalysts

Catalyst		I_D/I_{F2g}	O_v/%
$CuO–CeO_2$	n_{Cu}/n_{Ce}=0.4	0.087	4.64
	n_{Cu}/n_{Ce}=0.5	0.206	5.09
	n_{Cu}/n_{Ce}=0.6	0.274	6.61
	n_{Cu}/n_{Ce}=0.7	0.228	6.28
CeO_2		0.015	4.42

S5. Correlation of catalytic performance

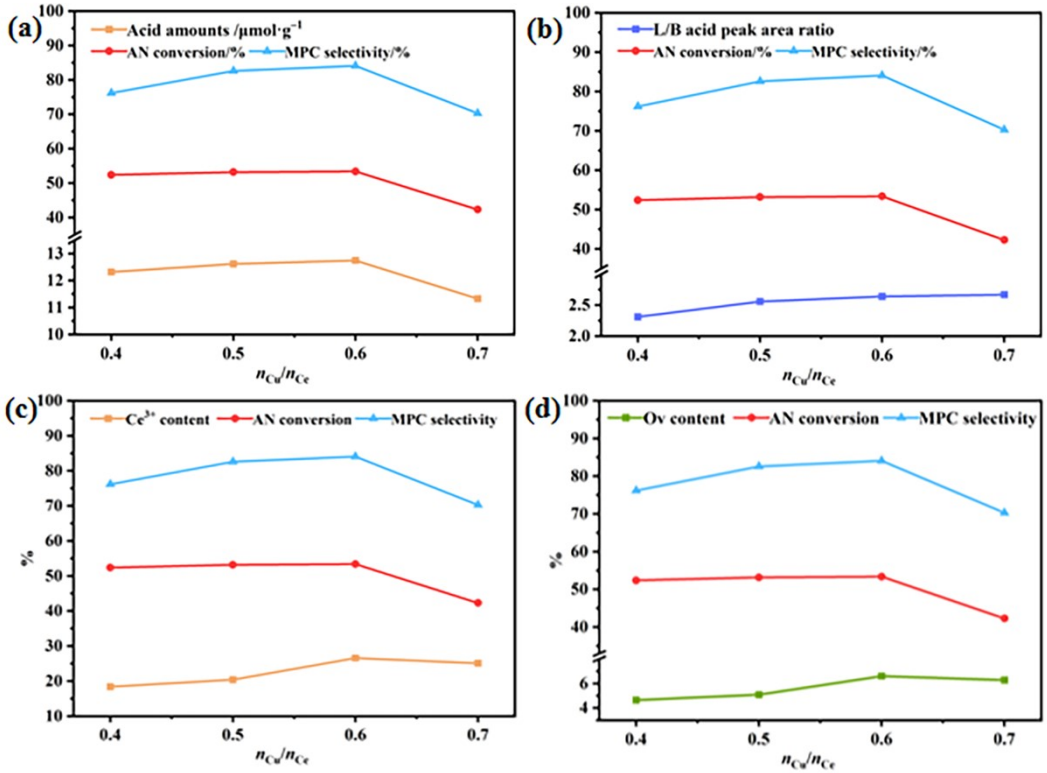

Fig. S4. The correlation between catalytic performance and the content of acid amounts (a), L/B acid peak area ratio (b), Ce^{3+} (c) and oxygen vacancies (d) level in CuO–CeO_2 with different n_{Cu}/n_{Ce}

S6. *In situ* FT-IR

Table S2 Absorption peaks and their corresponding functional groups in bare DMC and AN spectrum

substance	wavenumber cm^{-1}	functional group	vibrational mode	References
DMC	2965, 2865	$–CH_3$	C–H stretching vibration	[1]
	1460	$–CH_3$	C–H bending vibration	[2]
	1782, 1767	C=O	C=O stretching vibration	[3]
	1290	C–O–C	O–C stretching vibration	[3]
AN	1602, 1499	benzene ring	C=C stretching vibration	[4]
	3047	benzene ring	=C–H stretching vibration	[4]
	1620	$–NH_2$	N–H bending vibration	[5]
	3413, 3358	$–NH_2$	N–H stretching vibration	[5]

Table S3 Absorption peaks and their corresponding functional groups of DMC and AN absorbed on $CuO–CeO_2$ surface

substance	wavenumber cm^{-1}	functional group	vibrational mode	References
DMC	3378	–OH	O–H stretching vibration	[3]
	2910, 2811	$–OCH_3$	C–H stretching vibration	[6]
	1099	$–OCH_3$	O–C stretching vibration	[7]
	1036	$–OCH_3$	O–C stretching vibration	[7]
	1770, 1735	C=O	C=O stretching vibration	[2]
	1580	$–COOCH_3$	C=O stretching vibration	[8]
AN	3581	–OH	O–H stretching vibration	[3]
	1605	$–NH_2$	N–H bending vibration	[5]
	3348, 3270	$–NH_2$	N–H stretching vibration	[5]

S7. Catalytic performance of CuO–CeO_2 in MPC synthesis with error bars representing standard deviation (n=3)

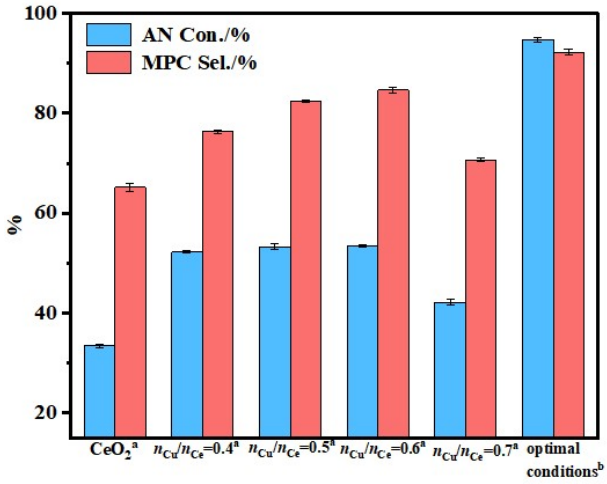

Fig. S5. Catalytic performances of diverse catalysts of MPC synthesis

[a]Reaction conditions: $n_{DMC}/n_{AN} = 20$, $m_{catal.}/m_{AN} = 0.25$, 150 °C, 7 h

[b]Reaction conditions: $n_{DMC}/n_{AN} = 10$, $m_{catal.}/m_{AN} = 0.25$, 170 °C, 9 h

References:

[1] H.T. Varghese, C.Y. Panicker, D. Philip, J.R. Mannekutla, S.R. Inamdar, IR, Raman and SERS studies of methyl salicylate, *Spectrochim. Acta A*, 2007, 66, 959–963.

[2] F. Li, Y. Jia, A.Z. Jia, L.Y. Gao, Y.J. Wang, Z.M. Wang, W. Xue, Fabrication and characterization of ZrO_2 and ZrO_2/SiO_2 catalysts and their application in the synthesis of methyl N-phenyl carbamate: a study of the reaction mechanism by using in situ FT-IR spectroscopy, *Reaction Kinetics, Mech. Catal.*,2021, 132, 893–906.

[3] Q.Y. Deng, L. Liu, H.M. Deng, Course of Spectral Analysis (2nd Ed.), Beijing: Science Press, 2007.

[4] J.Q. Fu, C.H. Ding, Study on alkylation of benzene with propylene over MCM-22 zeolite catalyst by in situ IR, *Catal. Commun.*, 2005, 6, 770–776.

[5] C. Gee, S. Douin, C. Crepin, P. Brechignac, Infrared spectroscopy of aniline ($C_6H_5NH_2$) and its cation in a cryogenic argon matrix, *Chem. Phys. Lett.*, 2001, 338, 130–136.

[6] P. Burg, P. Fydrych, D. Cagniant, G. Nanse, J. Bime, A. Jankowska, The characterization of nitrogen-enriched activated carbons by IR, XPS and LSER methods, *Carbon*, 2002, 40.

[7] C. Binet, M. Daturi, J.C. Lavalley, IR study of polycrystalline ceria properties in oxidised and reduced states, *Catal. Today*, 1999, 50, 207–225.

[8] R. Juarez, P. Concepcion, A. Corma, V. Fornes, H.Garcia, Gold-catalyzed phosgene-free synthesis of polyurethane precursors, *Angew. Chem. Int. Ed.*, 2010, 49, 1286–1290.